The Astrophysical Journal, 755:5 (8pp), 2012 August 10 doi:10.1088/0004-637X/755/1/5

DEEP SILICATE ABSORPTION FEATURES IN COMPTON-THICK ACTIVE GALACTIC NUCLEI PREDOMINANTLY ARISE DUE TO DUST IN THE HOST GALAXY

A. D. Goulding[1], D. M. Alexander[2], F. E. Bauer[3], W. R. Forman[1], R. C. Hickox[4], C. Jones[1], J. R. Mullaney[2,5], and M. Trichas[1]
[1] Harvard-Smithsonian Center for Astrophysics, 60 Garden Street, Cambridge, MA 02138, USA; agoulding@cfa.harvard.edu
[2] Department of Physics, University of Durham, South Road, Durham DH1 3LE, UK
[3] Departamento de Astronomia y Astrofisica, Pontificia Universidad Catolica de Chile, Casilla 306, Santiago 22, Chile
[4] Department of Physics and Astronomy, Dartmouth College, Hanover, NH 03755, USA
[5] Laboratoire AIM, CEA/DSM-CNRS-Universite Paris Diderot, Irfu/Service Astrophysique, CEA-Saclay, Orme des Merisiers, 91191 Gif-sur-Yvette Cedex, France
Received 2012 February 3; accepted 2012 May 31; published 2012 July 19

ABSTRACT

We explore the origin of mid-infrared (mid-IR) dust extinction in all 20 nearby ($z < 0.05$) bona fide Compton-thick ($N_{\rm H} > 1.5\times10^{24}$ cm^{-2}) active galactic nuclei (AGNs) with hard energy ($E > 10$ keV) X-ray spectral measurements. We accurately measure the silicate absorption features at $\lambda \sim 9.7$ μm in archival low-resolution ($R \sim 57$–127) *Spitzer* Infrared Spectrograph spectroscopy, and show that only a minority (≈45%) of nearby Compton-thick AGNs have strong Si-absorption features ($S_{9.7} = \ln(f_{\rm int}/f_{\rm obs}) \gtrsim 0.5$) which would indicate significant dust attenuation. The majority (≈60%) are star formation dominated (AGN:SB < 0.5) at mid-IR wavelengths and lack the spectral signatures of AGN activity at optical wavelengths, most likely because the AGN emission lines are optically extinguished. Those Compton-thick AGNs hosted in low-inclination-angle galaxies exhibit a narrow range in Si-absorption ($S_{9.7} \sim 0$–0.3), which is consistent with that predicted by clumpy-torus models. However, on the basis of the IR spectra and additional lines of evidence, we conclude that the dominant contribution to the observed mid-IR dust extinction is dust located in the host galaxy (i.e., due to disturbed morphologies, dust lanes, galaxy inclination angles) and not necessarily a compact obscuring torus surrounding the central engine.

Key words: galaxies: active – galaxies: Seyfert – infrared: galaxies – X-rays: galaxies

Online-only material: color figures

1. INTRODUCTION

The unified model of active galactic nuclei (AGNs; e.g., Antonucci 1993) is crucial to our understanding of the growth and evolution of massive black holes and their host galaxies. A key issue in AGN physics is the nature of the obscuring medium surrounding the central engine.

There are three competing models for the specific structure, geometry, and composition of the obscuring material surrounding the central supermassive black hole (SMBH): (1) a uniform (smooth/continuous), heavily obscuring, sub-parsec scale torus (Pier & Krolik 1992, 1993); (2) an extended torus yielding moderate obscuration (Granato & Danese 1994; Efstathiou & Rowan-Robinson 1995; Granato et al. 1997); and (3) a clumpy "torus" of many individual optically thick clouds (Nenkova et al. 2002, 2008). Each of these theoretical models make clear predictions for the observed torus properties. The graphite/silicate dust contained within the torus is predicted to extinguish AGN emission at UV/optical wavelengths, and should be cospatial with cool neutral gas which readily absorbs the X-ray emission from the AGN (e.g., Mushotzky et al. 1993). However, this dust/gas-rich torus is also predicted to (isotropically) re-emit in the mid-infrared (mid-IR, $\lambda \sim 5$–50 μm) with a mid-IR spectral energy distribution characterized by a power-law-like AGN continuum, superposed with silicate absorption/emission features at 9.7 μm and 18 μm. The strength of these dust features is expected to be dependent on the specific geometry and optical depth of the torus (e.g., Fritz et al. 2006; Schartmann et al. 2008). To distinguish between these torus models, we require well-constrained results from sensitive and high-quality observations.

In nearby optical and radio-selected AGNs, a weak correlation between gas column density ($N_{\rm H}$) and silicate (Si) absorption strength has been observed from *Spitzer* mid-IR spectroscopy (e.g., Shi et al. 2006; Wu et al. 2009). In turn, this suggests that selection of sources with strong Si-absorption is a good method to find the most heavily obscured AGNs, i.e., Compton-thick sources with $N_{\rm H} > 1.5 \times 10^{24}$ cm^{-2} (e.g., Georgantopoulos et al. 2011). To first order, these results would appear to agree with those predicted by simple uniform torus models. However, there is growing evidence that not all of the dust extinction can be attributed to an obscuring central torus.

Using ground-based high spatial resolution photometry, Gandhi et al. (2009) show that Compton-thick AGNs do not require significant corrections for dust extinction to their AGN-produced mid-IR continuum, suggesting that Si-absorption features in Compton-thick AGNs are not being produced in their nuclear regions (see also Hönig et al. 2010; Asmus et al. 2011). Furthermore, those AGNs with strong Si-absorption features are often found to be hosted in highly inclined and/or merging galaxies (e.g., Deo et al. 2007, 2009), providing first-order evidence that significant dust attenuation can occur within the AGN host galaxy (e.g., Alonso-Herrero et al. 2011, and references therein). Moreover, dust in the host galaxy appears to extinguish the optical emission-line signatures in ≈25%–50% of nearby AGNs (e.g., Goulding & Alexander 2009), and in a minority of cases, even the mid-IR AGN emission lines (e.g., NGC 4945; Goulding et al. 2010). This apparent ambiguity among recent observations and theory raises two fundamental questions. (1) Is Si-absorption a common feature among Compton-thick AGNs, as predicted by a unified AGN model? (2) Does Si-absorption predominantly arise from dust in a central torus or from within the AGN host galaxy?

To address these questions we explore the origins of apparent high optical-depth dust in the sample of all 20 nearby ($z \lesssim 0.05$) Compton-thick AGNs which are unambiguously identified

with high-energy X-ray spectral observations. We use *Spitzer* Infrared Spectrograph (IRS) observations to determine the average mid-IR spectral energy distribution of Compton-thick AGNs, and establish whether silicate absorption is a signature common to the most heavily obscured AGNs. In Section 2 we describe the sample of Compton-thick AGNs, outline the data reduction methods of the *Spitzer*-IRS observations, and present the mid-IR spectra for the Compton-thick AGN sample. In Section 3 we compare the absorbing gas column and the apparent dust-extinction levels toward the central AGN and present the physical implications of these in light of a clumpy-torus model. Finally, in Section 4 we review our results, finding that the mid-IR Si-absorption features observed in Compton-thick AGNs are produced primarily due to dust in the AGN host galaxy and not within a central torus.

2. COMPTON-THICK AGN SAMPLE AND DATA ANALYSES

Compton-thick AGNs ($N_{\rm H} > 1.5 \times 10^{24}$ cm^{-2}) are the most heavily obscured class of AGNs; by their very nature, they are extremely difficult to detect and remain hidden in most X-ray surveys (e.g., Norman et al. 2002; Alexander et al. 2008, 2011; Comastri et al. 2011; Feruglio et al. 2011; Gilli et al. 2011; Luo et al. 2011). Conclusive identifications of Compton-thick AGNs are made through spectroscopic X-ray observations performed at $E > 10$ keV, where the relatively unabsorbed high-energy emission can be directly detected. The current sensitivities of $E > 10$ keV observatories (e.g., *BeppoSAX*, *Swift*, *Suzaku*, *INTEGRAL*) are substantially limited by high backgrounds, relatively small effective areas, and low spatial resolution. To date, only 20 bona fide Compton-thick AGNs have been unambiguously identified in the universe at $E > 10$ keV (for a review see Della Ceca et al. 2008, and references therein; Awaki et al. 2009; Braito et al. 2009). These 20 Compton-thick AGNs are all nearby ($z \lesssim 0.05$) systems hosted in spiral (Hubble-type S0 or later) or merging galaxies with intrinsic X-ray luminosities $L_{\rm X,intrinsic} \sim (0.06\text{–}200) \times 10^{42}$ erg s^{-1} ($E \sim 2\text{–}10$ keV), and hence span the wide range of AGN power observed in local Seyfert systems.

2.1. Spitzer-IRS Data Reduction

All 20 bona fide Compton-thick AGNs identified to date have archival low-resolution *Spitzer*-IRS spectroscopy. Specifically, these 20 AGNs have been observed with the low-resolution modules (short–low (SL, 5.2–14.5 μm) and long–low (LL, 14.0–38.0 μm); $R \approx 57\text{–}127$) in either staring or mapping mode as part of multiple programs, and hence these data form a heterogeneous, but still complete sample. Our sample of nearby Compton-thick AGNs and their basic properties are given in Table 1. The mid-IR data for many of our AGN sample have been analyzed using different reduction techniques in previous papers (e.g., Deo et al. 2007; Hao et al. 2007; Wu et al. 2009; Mullaney et al. 2010, 2011; S. Sazonov et al. 2012, submitted). However, in order to ensure self-consistency for the measurement of the spectral absorption/emission features which are integral to the analyses presented here, we have re-extracted each of the IRS observations using our own custom IDL reduction routine (see Goulding 2010; Goulding et al. 2011; Mullaney et al. 2011).

Briefly, the two-dimensional Basic Calibrated Data (BCDs) images, produced by the S18.18.0 Spitzer Science Center (SSC) pipeline, were retrieved and rigorously cleaned of rogue "hot" pixels using our customized version of IRSCLEAN. Next, individual rows were fitted as a function of time to remove latent charge which exists on the detector after bright and/or long observations. The IRS Staring observations were averaged in the different nod positions, which were then used to perform alternate background subtractions of the source in each nod position and final spectra were extracted using the *Spitzer*-IRS Custom Extraction (SPICE) software provided by the SSC. Cleaned and processed IRS Mapping observations were input to the SSC package CUBISM to build the spectral data cubes and extract the one-dimensional (1D) spectroscopy. Individual IRS orders in the 1D spectra were clipped of noise (see the *Spitzer*-IRS handbook for further information) and stitched together by fitting low-order polynomials to produce the final continuous spectra for each source. In the upper panel of Figure 1, we show the resulting low-resolution *Spitzer*-IRS spectroscopy for our complete sample of nearby Compton-thick AGNs.

2.2. Spitzer-IRS Spectral Decomposition and Silicate Absorption Measurement

On the basis of uniform dust torus models produced from radiative transfer theory (e.g., Dullemond & van Bemmel 2005; Schartmann et al. 2005; Fritz et al. 2006), the mid-IR spectral energy distributions of intrinsically heavily absorbed Type-2 AGNs are expected to be dominated by an AGN-produced power law and most, if not all, are expected to exhibit significant Si-absorption features at $\lambda \sim 9.7\,\mu$m. Throughout this manuscript, we define $S_{9.7}$ as the depth of the Si-absorption feature at $\lambda \sim 9.7\,\mu$m where $S_{9.7} = \ln(f_{9.7,\rm intrinsic}/f_{9.7,\rm observed})$. Following many previous studies, we use $S_{9.7}$ as a good proxy for the apparent optical depth and dust extinction in our sample (e.g., Spoon et al. 2007; Shi et al. 2006; Levenson et al. 2007; Deo et al. 2007, 2009; Georgantopoulos et al. 2011). Though we note that the relation between $S_{9.7}$ and true optical depth is most likely nonlinear and somewhat model and orientation dependent (see Levenson et al. 2007; Nenkova et al. 2008; Schartmann et al. 2008).

Previous investigations have often employed simple extrapolation methods to estimate the depth of the silicate feature in mid-IR spectroscopy (e.g., Spoon et al. 2007; Levenson et al. 2007; Georgantopoulos et al. 2011). This involves measurement of the observed continuum blueward and redward of the silicate feature, extrapolating a power law between the continuum points and comparing this to the observed flux at $\lambda \sim 9.7\,\mu$m. In principle, this extrapolation method is sufficient for AGN-dominated spectra. However, as shown in Figure 1, the majority of the mid-IR spectra for Compton-thick AGNs contain strong polycyclic aromatic hydrocarbon (PAH) features (at 6.3, 7.7, 11.3, and 12.3 μm) indicative of substantial circumnuclear star formation activity. These PAH features provide significant contributions to the mid-IR spectra blueward of the Si-absorption feature, having the effect of artificially increasing the continuum strength at $\lambda \sim 6\text{–}8\,\mu$m and, hence, overestimating the intrinsic AGN continuum flux at $\lambda \sim 9.7\,\mu$m. In a pure synthetic star-forming template with *no* evidence for extinction, a substantial Si-absorption feature ($S_{9.7} \sim 0.7$) would be inferred using this basic method. Therefore, we choose to use a spectral decomposition method to remove the host-galaxy emission, and measure the depth of the Si-absorption feature only within the AGN component. Furthermore, to constrain any systematic uncertainties derived from using any one spectral decomposition method we use two independent spectral decomposition procedures.

First, we use the IDL software package `DecompIR` (Mullaney et al. 2011), which performs a chi-squared minimization of

Table 1
The Compton-thick AGN Sample

Common Name	α_{J2000}	δ_{J2000}	z	D_L (Mpc)	Gal. Morph.	b/a	D L/ Pec.	Opt. Class	$L_{X,corr}$ (erg s^{-1} cm^{-2})	N_H ($\times 10^{24}$ cm^{-2})	X-Ray Ref.	IRS Type	AOR No.	Obs. Date	$S_{9.7}$ DecompIR	$S_{9.7}$ PAHFIT	Mid-IR AGN:SB Ratio
(1)	(2)	(2)	(3)	(4)	(5)	(6)	(7)	(8)	(9)	(10)	(11)	(12)	(13)	(14)	(15)	(16)	(17)
NGC 424	$01^h11^m27\overset{s}{.}6$	$-38^d05^m00^s$	0.0125	50.8	SBa	0.45	...	Sy1/2	42.63	$3.5^{+1.8}_{-1.4}$	1,2	M	12444160	2004 Dec 8	<0.00	0.00	>0.9
NGC 1068	$02^h42^m40\overset{s}{.}7$	$-00^d00^m47^s$	0.0116	13.7	SAb	0.85	...	Sy2	>41.71	>10.0	3,4,5,6,7	M	12461568	2005 Jan 12	0.08	0.12	>0.9
E005-G004	$06^h05^m41\overset{s}{.}6$	$-86^d37^m55^s$	0.0062	26.7	Sb	0.21	...	H II	41.92	$1.6^{+0.5}_{-0.4}$	8	S	18947328	2006 Oct 25	0.61	0.47	0.60
Mrk3	$06^h15^m36\overset{s}{.}4$	$+71^d02^m15^s$	0.0134	60.6	S0	0.89	...	Sy2	43.51	$1.3^{+0.2}_{-0.2}$	9,10,11	S	3753472	2004 Mar 4	0.33	0.15	>0.9
NGC 2273	$06^h50^m08\overset{s}{.}7$	$+60^d50^m44^s$	0.0038	26.5	SBa	0.78	...	Sy2	42.23	~1.5	12	S	4851712	2004 Oct 3	0.24	0.20	0.49
NGC 3079	$10^h01^m57\overset{s}{.}8$	$+55^d40^m47^s$	0.0061	16.2	SBc	0.18	...	L/Sy2	42.10	$10.0^{+10.0}_{-5.3}$	13	S	3755520	2004 Apr 19	0.65	0.58	0.32
NGC 3281	$10^h31^m52\overset{s}{.}1$	$-34^d51^m13^s$	0.0038	49.6	SAab	0.52	Y	Sy2	43.17	$2.0^{+0.2}_{-0.1}$	4,10,14	S	4852224	2005 May 23	1.41	1.28	0.87
NGC 3393	$10^h48^m23\overset{s}{.}5$	$-25^d09^m43^s$	0.0115	56.2	SB0	0.91	...	Sy2	>42.85	>10.0	7,15	S	4852480	2005 May 22	0.13	0.14	0.77
Arp299	$11^h28^m30\overset{s}{.}4$	$+58^d34^m10^s$	0.0110	44.8	Irr	...	Y	H II	42.84	$2.5^{+1.4}_{-0.6}$	16,17	M	3840256	2004 Apr 15	0.90	0.92	0.63
Mrk231	$12^h56^m14\overset{s}{.}2$	$+56^d52^m25^s$	0.0420	186.0	SAc	0.77	...	QSO	43.70	~2.0	18	S	4978688	2004 Apr 14	0.18	0.13	0.77
NGC 4939	$13^h04^m14\overset{s}{.}4$	$-10^d20^m22^s$	0.0104	44.8	SAbc	0.51	...	Sy2	>42.63	>10.0	15	S	4853760	2004 Jan 6	0.00	0.00	>0.9
NGC 4945	$13^h05^m27\overset{s}{.}5$	$-49^d28^m05^s$	0.0019	3.9	Scd	0.19	Y	H II	42.30	$2.2^{+0.3}_{-0.4}$	4,5,6,19	S	8768928	2004 Mar 1	1.40	0.74	<0.2
NGC 5194	$13^h29^m52\overset{s}{.}7$	$+47^d11^m42^s$	0.0015	8.6	SAbc	0.99	...	L/Sy2	40.76	$5.6^{+4.0}_{-1.6}$	20	M	9480192	2004 May 12	0.00	0.04	0.43
Circinus	$14^h13^m09\overset{s}{.}9$	$-65^d20^m20^s$	0.0014	3.7	SAb	0.43	Y	Sy2	41.90	$4.3^{+0.4}_{-0.7}$	11,21,22	S	9074176	2004 Mar 1	1.28	1.25	0.88
NGC 5728	$14^h42^m23\overset{s}{.}9$	$-17^d15^m11^s$	0.0094	40.9	SABa	0.58	...	Sy2	43.04	$2.1^{+0.2}_{-0.2}$	10,23	S	18945536	2007 Aug 5	0.14	0.12	0.52
E138-G001	$16^h51^m20\overset{s}{.}1$	$-59^d14^m05^s$	0.0091	38.6	S0	0.99	...	Sy2	42.52	~1.5	2,6	S	17643264	2007 Apr 30	0.00	0.00	>0.9
NGC 6240	$16^h52^m58\overset{s}{.}9$	$+02^d24^m03^s$	0.0243	105.0	Irr	...	Y	L	44.26	$2.2^{+0.4}_{-0.3}$	11,24	S	4985600	2004 Mar 4	0.82	0.62	0.44
IRAS19254-7245	$19^h31^m21\overset{s}{.}4$	$-72^d39^m18^s$	0.0620	266.0	Irr	...	Y	QSO	44.50	$3.1^{+1.2}_{-0.4}$	27	S	12256512	2005 May 30	1.07	0.58	0.64
NGC 7582	$23^h18^m23\overset{s}{.}5$	$-42^d22^m14^s$	0.0053	22.7	SBab	0.42	Y	Sy2	42.61	$1.6^{+0.9}_{-0.5}$	10,25	M	12445184	2005 May 25	0.76	0.79	0.37
NGC 7674	$23^h27^m56\overset{s}{.}7$	$+08^d46^m44^s$	0.0289	127.0	SAbc	0.91	...	Sy2	>43.34	>10.0	26	M	12468736	2004 Dec 11	0.10	0.00	>0.9

Notes. [1]Common galaxy name; [2]J2000 positional coordinates from the NASA Extragalactic Database (NED); [3]spectroscopic redshift; [4]luminosity distance in megaparsecs assuming $H_0 = 71\,\mathrm{km\,s^{-1}\,Mpc^{-1}}$ and $\Omega_\Lambda = 0.70$ and corrected for non-cosmological flows; [5 and 6]galaxy morphology and major/minor axis ratio taken from the Third Reference Catalog of Bright Galaxies (de Vaucouleurs et al. 1991); [7]Y denotes dust lanes or peculiar morphology are evident in the optical image of the source; [8]optical classification in NED; [9]logarithm of intrinsic (2–10 keV) X-ray luminosity in units of erg s^{-1} corrected for Compton-thick absorption for those sources with $N_H < 10^{25}$ cm^{-2}; [10]neutral hydrogen column density derived from hard X-ray spectroscopy in units of 10^{24} cm^{-2}; [11]reference for X-ray data (see below); [12]type of *Spitzer*-IRS observation (M: mapping; S: staring); [13]*Spitzer* observation record indicator; [14]date of *Spitzer*-IRS observation; [15]depth of Si-absorption at $\lambda \sim 9.7\,\mu$m derived from spectral fits to *Spitzer*-IRS data using the formalism of Mullaney et al. (2011); [16]depth of Si-absorption at $\lambda \sim 9.7\,\mu$m derived from spectral fits to *Spitzer*-IRS data using PAHFIT; [17]AGN–starburst ratio derived from fitting IRS spectrum with DecompIR (AGN-dominated system = 1).

References. (1) Iwasawa et al. 2001; (2) Collinge & Brandt 2000; (3) Matt et al. 1997; (4) Sazonov et al. 2007; (5) Beckmann et al. 2006; (6) Bassani et al. 2007; (7) Levenson et al. 2006; (8) Ueda et al. 2007; (9) Cappi et al. 1999; (10)Markwardt et al. 2005; (11) Bassani et al. 1999; (12) Awaki et al. 2009; (13) Iyomoto et al. 2001; (14) Vignali & Comastri 2002; (15) Maiolino et al. 1998; (16) Della Ceca et al. 2002; (17) Ballo et al. 2004; (18) Braito et al. 2004; (19) Guainazzi et al. 2000; (20) Fukazawa et al. 2001; (21) Matt et al. 1999; (22) Iwasawa et al. 1997; (23) Comastri et al. 2007; (24) Vignati et al. 1999; (25) Turner et al. 2000; (26) Malaguti et al. 1998; (27) Braito et al. 2009.

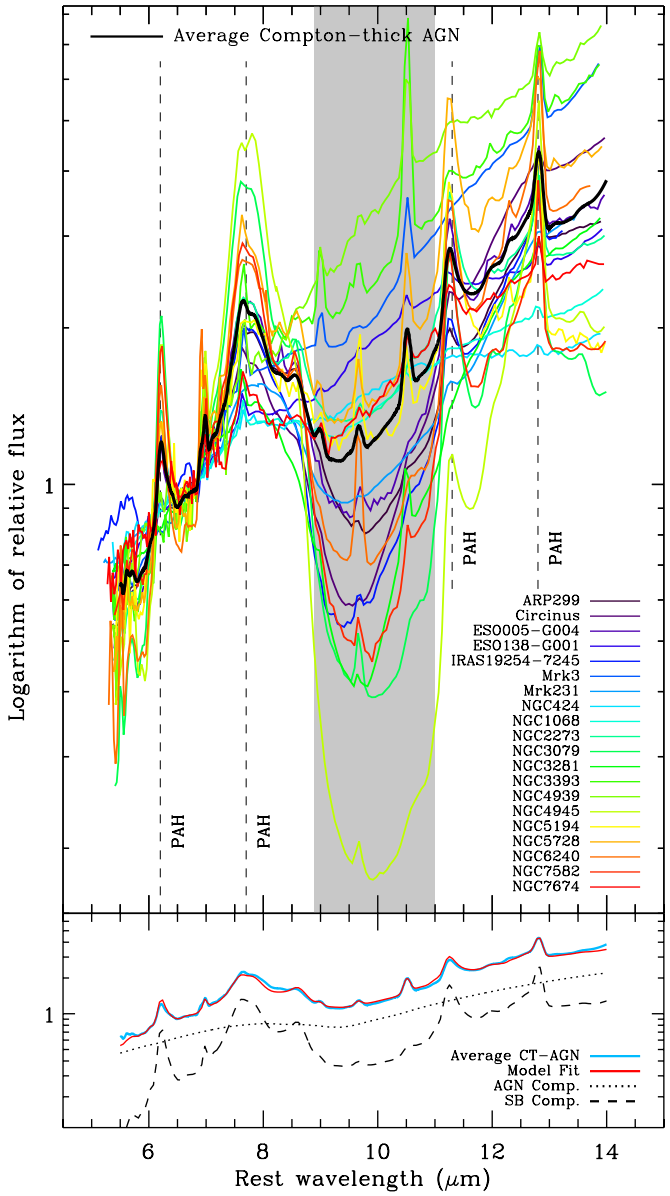

Figure 1. Upper panel: low-resolution ($R \sim 57$–127) *Spitzer*-IRS spectroscopy of all 20 bona fide Compton-thick AGNs in the nearby universe with high-energy ($E > 10$ keV) spectroscopic constraints. The gray shaded region represents the wavelength boundaries for the dominant Si-absorption feature ($\lambda \sim 9.7\,\mu$m) in the short–low (SL) *Spitzer*-IRS passband. The mid-IR spectral energy distributions of Compton-thick AGNs are clearly very diverse with spectra dominated by a combination of an AGN-produced power law; strong starburst-produced polycyclic aromatic hydrocarbon features at $\lambda \sim 6.3$, 7.7, 11.3, and 12.8 μm; and in a *minority* (9/20) of cases, strong ($S_{9.7} > 0.3$) Si-absorption features. Additionally, we show the average mid-IR spectrum of the sample of Compton-thick AGNs (thick black line). Lower panel: spectral decomposition of the average Compton-thick AGN spectrum (blue solid curve). The best-fit extinction-convolved AGN power law and starburst templates are shown with dotted and dashed curves, respectively. The total best-fit spectrum (i.e., power law + starburst + emission lines) is shown with a solid red curve. The best-fitting constraints for various AGN classifications are given in Table 2.

(A color version of this figure is available in the online journal.)

the observed spectrum to a combination of starburst templates (i.e., a host-galaxy component) and an absorbed power law (i.e., an AGN component). Here, we employ a simple screen extinction curve (Draine 2003) to account for absorption of the AGN component; thus, we do not attempt to constrain the physical region where dust extinction is occurring. Following Goulding et al. (2011), we allow for a range of star-forming templates, including that of the archetypal nearby starburst, M82; a combined Brandl et al. (2006) starburst template;[6] and a range of compact nuclear and extranuclear theoretical starburst templates (Siebenmorgen & Krügel 2007). From the fitted AGN component, we predict the intrinsic power of the AGN at $\lambda \sim 9.7\,\mu$m, and compare this to the observed luminosity to establish an estimate for $S_{9.7}$ (Column 15 of Table 1). Second, we employ the widely used spectral-fitting package, PAHFIT (Smith et al. 2007) to fit a range of heated dust continua combined with PAH and emission-line features to derive $S_{9.7}$ (Column 16 of Table 1). Following Georgantopoulos et al. (2011), we change the default dust continuum temperatures in PAHFIT and additionally allow hotter dust temperatures (400–1400 K) to be fitted to the spectra; these are expected to arise from an accretion-heated AGN torus. In general, we find very good agreement for $S_{9.7}$ derived using DecompIR and PAHFIT (see Columns 15 and 16 of Table 1). In Section 3, we compare these two measures of the Si-absorption feature to gas column density in Compton-thick AGNs.

2.3. The Average Mid-IR Spectra of Compton-thick AGNs

In Figure 1 we show that Compton-thick AGNs at $z \sim 0$ are characterized by a variety of spectral shapes with AGN–starburst ratios of ∼0.1–1. Of the 20 AGNs in our sample, only four appear to be dominated by a featureless power-law continuum, while eleven show strong PAH features indicative of circumnuclear starburst activity which, for seven (≈35%) of the sources, even dominates the bolometric output of the galaxies at mid-IR wavelengths (AGN:SB $\lesssim$ 0.5; see Column 17 of Table 1). By contrast, S. Sazonov et al. (2012, submitted) find that only $\lesssim$20% of all hard X-ray-selected Compton-thin ($N_{\rm H} \sim (0.05$–$100) \times 10^{22}$ cm^{-2}) Type-2 AGNs detected by *INTEGRAL* are dominated by star formation at mid-IR wavelengths. It is therefore possible that enhanced star formation activity may be a characteristic specific to the most heavily absorbed ($N_{\rm H} > 10^{24}$ cm^{-2}) AGNs, and not merely a hard X-ray selection effect, at least in the nearby universe.

Through spectral stacking, we find that Compton-thick AGNs, on average, show strong star formation activity. We stacked all 20 mid-IR spectra to produce a mean mid-IR spectral energy distribution for Compton-thick AGNs. We chose to normalize the rest-frame mid-IR spectra for each of the Compton-thick AGNs at $\lambda \sim 6.5$–$7\,\mu$m (i.e., a wavelength range with a relatively featureless continuum). In the lower panel of Figure 1, we show the spectral decomposition of the average spectrum modeled using DecompIR. Our modified Brandl et al. (2006) template provides the best χ^2-fit "starburst" to the mean Compton-thick AGN spectrum, and contributes ≈40% of the overall luminosity to Compton-thick AGN at mid-IR wavelengths.

As we show in Table 1 and Figure 1, the detection of Si-absorption features in nearby Compton-thick AGNs is far from ubiquitous. The Compton-thick AGNs cover a wide range in Si-absorption depth, $S_{9.7} \sim 0$–1.4. While the mid-IR spectra for eight of the Compton-thick AGNs do appear to be moderately extinguished, we also find that the spectral decomposition (using DecompIR) of NGC 424 shows strong evidence for Si-*emission* ($S_{9.7} < 0.0$); based on unified models, Si-emission features

[6] We do not include NGC 660, NGC 1365, NGC 3628, and NGC 4945 as part of the Brandl et al. (2006) template as these sources are known to harbor AGNs.

are expected only in unobscured Type-1 AGNs, irrespective of specific torus geometry/composition. This result is also partially confirmed by PAHFIT which produces a relatively poor fit ($\chi^2_{n-1} \sim 26.1$) for NGC 424 and by design does not allow apparent optical depths of $S_{9.7} < 0.0$. Explanations for Si-emission features in Type-2 AGNs (e.g., NGC 2110, Mason et al. 2009; SST1721+6012, Nikutta et al. 2009) are that the emission is either (1) arising from the innermost region of the AGN narrow-line region, above the scale height of the torus (Mason et al. 2009); or (2) from an unobscured inner region of a low-mass clumpy torus (e.g., based on the models of Schartmann et al. 2008).

From the AGN power-law component of the stacked Compton-thick AGN spectrum, we directly measure the depth of the Si-absorption feature at $\lambda \sim 9.7\,\mu$m. We find that, on average, the re-radiated AGN emission of a Compton-thick source experiences an apparent attenuation of only $S_{9.7} \sim 0.36 \pm 0.04$, equivalent to an optical extinction of $A_V \approx 3.9$–4.9 mag.[7] Optical depths such as these are readily observed in nearby galactic star-forming regions (e.g., Draine 2003). In Section 3.2, we further explore whether this measured dust extinction in Compton-thick AGNs can be attributed only to that arising in the host galaxy and not necessarily from an obscuring torus.

3. GAS ABSORPTION AND DUST EXTINCTION IN COMPTON-THICK AGNs

Unified AGN models postulate that obscuring gas and dust are both located in the circumnuclear torus, so that large gas columns are associated with heavy dust extinction and, for a uniform torus, deep Si-absorption features. With this in mind, a number of recent studies use the existence of high apparent optical depth ($S_{9.7} > 1$) to identify Compton-thick AGNs (e.g., Georgantopoulos et al. 2011; Nardini & Risaliti 2011; Dasyra et al. 2011). However, as shown in Figure 1, the large range in $S_{9.7}$ seen across our complete Compton-thick AGN sample suggests that the dust producing the Si-absorption features may not be cospatial with the X-ray absorbing gas.

3.1. Compton-thick AGNs with Little Apparent Dust Extinction

To establish if a physical link exists between the gas and dust in Compton-thick AGNs, as expected by a unified model, in this section we compare the depth of the Si-absorption feature and the gas column density. In Figure 2, we plot the measured X-ray gas column density versus mid-IR Si-absorption strength ($S_{9.7}$). For each AGN, we use the average value for $S_{9.7}$ derived independently from DecompIR and PAHFIT in the previous section. Error bars represent the spread in the values of $S_{9.7}$ for a particular source. We find little or no observed correlation between gas absorption and dust extinction in Compton-thick AGNs (Spearman's rank $\rho \sim -0.30$, $P_{\rm null} \sim 0.21$). At least eight of the sources exhibit little or no evidence for dust extinction ($S_{9.7} \lesssim 0.1$) and, moreover, NGC 424 has silicate *emission* features ($S_{9.7} < 0.0$); in general, such emission features require a direct line of sight to the inner AGN torus. By contrast, 9 of the 20 ($\sim$45% $\pm$ 18%) Compton-thick AGNs in our sample appear moderately ($S_{9.7} \sim 0.5$–1.0) to heavily ($S_{9.7} > 1.0$) obscured at mid-IR wavelengths, as would be expected by unified AGN models that invoke a smooth uniform dust torus. However, the fraction of Compton-thick AGNs

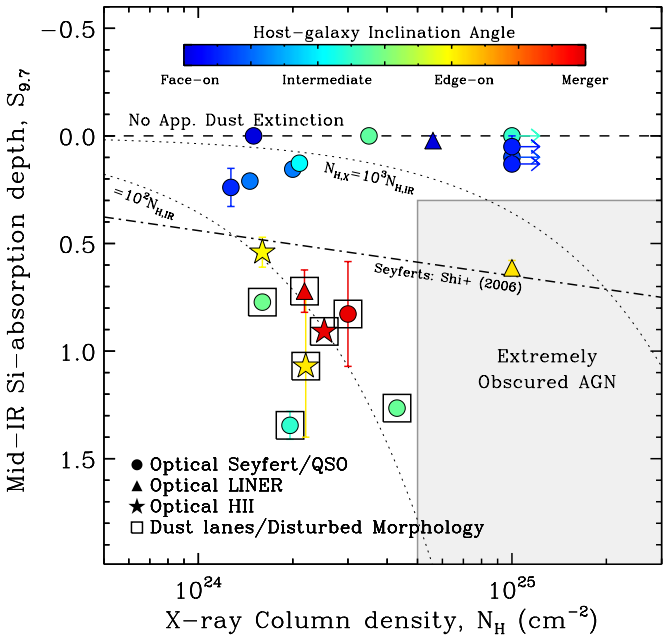

Figure 2. Si-absorption depth at 9.7 μm ($S_{9.7}$, a good proxy for apparent dust extinction) observed in *Spitzer*-IRS mid-IR spectroscopy vs. hard X-ray-derived gas column density ($N_{\rm H}$) in units of cm^{-2} for all bona fide Compton-thick AGNs in the nearby universe. Error bars represent the range in $S_{9.7}$ measured using DecompIR and PAHFIT. Constant gas–dust ratios are shown (dotted lines) for ratios of $N_{\rm H,X}/N_{\rm H,IR} = 100$ and 1000 assuming $N_{\rm H}/A_V = 1.93 \times 10^{21}$ cm^{-2} and $A_{9.7}/A_V \simeq 0.075$ (e.g., Draine & Li 2007). Inclination angles are shown with color gradient and are derived from major–minor axis ratios (see Column 6 of Table 1): face-on systems ($b/a \sim 1$) are shown in blue, edge-on ($b/a \sim 0$) in yellow, colors in between are linearly scaled to intermediate inclination angles ($b/a \sim 0$–1), and merging systems (established from optical imaging and NED classifications) are shown in red. Optical spectral classifications (AGN, LINER, H II/star forming) are shown with filled circles, triangles, and stars, respectively. Additionally, sources with dust lanes or disturbed optical morphologies are highlighted with open squares (see Column 7 of Table 1). For comparison, we show the linear fit presented in Shi et al. (2006) for a sample of Seyfert galaxies with measured $N_{\rm H}$.

(A color version of this figure is available in the online journal.)

with high apparent optical depth ($S_{9.7} \gtrsim 0.5$) is similar to that measured for lower column density ($N_{\rm H} \sim$ (0.05–50) $\times$ 10^{22} cm^{-2}) AGNs detected by *Swift*-BAT, 30% $\pm$ 10% (derived from the spectroscopy presented in Mullaney et al. 2010), suggesting that large $N_{\rm H}$ does not necessarily predicate large dust extinction. Indeed, at least four ($\approx$10%) Compton-thin *Swift*-BAT AGNs presented in Mullaney et al. (2010) have $S_{9.7} \gtrsim 1$.

In Figure 2 we additionally show curves of constant gas column density predicted using $S_{9.7}$ assuming a standard optical–IR Milky Way extinction curve (Draine & Li 2007) and a gas–dust ratio of $N_{\rm H}/A_V = 1.93 \times 10^{21}$ cm^{-2} mag^{-1} (Fitzpatrick 1985; Draine 2003 for $R_V = A_V/E(B-V) = 3$). We show that Compton-thick AGNs are required to have gas–dust ratios which are a factor $\approx$50–10,000 greater than observed galactically, which may suggest that there is no single gas–dust ratio in these sources (e.g., Maiolino et al. 2001). These large gas–dust ratios may be explained by additional absorption of X-ray emission by large quantities of neutral gas residing within the dust-sublimation radius ($0.1 < r < 10$ pc) of the obscuring torus, so-called partial covering.

Recent X-ray monitoring campaigns of variable absorption state AGNs (e.g., Mrk766, NGC 1365, NGC 4151) have observed short-term occultations of the X-ray source by high-velocity ($\sim$3000 km s^{-1}) circumnuclear gas clouds residing at

[7] Throughout we assume a standard optical–IR extinction curve (Draine & Li 2007) in the direction of the Milky Way galactic center such that $A_{9.7\,\mu{\rm m}}/A_V \simeq 0.075$.

~0.1 pc (e.g., Risaliti et al. 2009a, 2009b; Wang et al. 2010). The motion and distance from the central source of these gas clouds are consistent with that expected for X-ray absorption arising from the AGN broad-line region (BLR; e.g., Risaliti et al. 2009a, 2011). Within these relatively small radii, SiO dust grains are preferentially destroyed due to the high temperatures ($T > 1000$ K). Hence, the gas–dust ratio of the BLR may be far larger than that of the dusty torus. However, partial covering may not explain the high gas–dust ratio observed in all of the Compton-thick AGNs included here. Recent, spatially resolved results of Marinucci et al. (2012) suggest that at least a fraction of the Compton-thick gas clouds in NGC 4945 may reside at far larger radii (~100 pc) than the BLR. These variations in BLR and torus absorptions as well as inclination effects (e.g., Nenkova et al. 2008) may add substantial scatter to an expected gas–dust ratio for nearby AGNs. Taken together, these results give rise to several interesting scenarios for: (1) the spatial extent of the intervening gas and dust, (2) the density gradient of the materials across the torus, and (3) possible gas–dust separation boundaries within a torus. Given our small sample and (by design) our limited range in $N_{\rm H}$, these issues are beyond the scope of this investigation. We may still robustly conclude that all Compton-thick AGNs (i.e., large $N_{\rm H}$ sources) are *not* necessarily obscured by cool dust with high apparent optical depth. However, the reverse of this statement may still also be true, in that all systems observed to have $S_{9.7} \gg 1$ may all contain Compton-thick AGNs, but are currently missed due to the lack of sufficiently sensitive instrumentation; although these extreme $S_{9.7} \gg 1$ sources are only a limited sub-set (<20%) of the Compton-thick AGN population.

3.2. Evidence for Dust Extinction Arising in the Host Galaxy of Compton-thick AGNs

The apparent lack of a correlation between gas and dust attenuation in Compton-thick AGNs presented in the previous section suggests that the gas and dust may not be cospatial. Indeed, Sturm et al. (2005) suggested an extranuclear origin for the Si-absorption features observed in both low- and high-luminosity AGNs. This is supported by Gandhi et al. (2009) who showed in high spatial resolution ground-based photometry of nuclear regions in nearby AGNs that the AGN-produced mid-IR continuum appears almost isotropic and unaffected by Si-absorption. Furthermore, the inclination angle of the host galaxy may have a significant obscuring effect on the AGN emission (e.g., Malkan et al. 1998; Matt et al. 2000; Alonso-Herrero et al. 2011; Lagos et al. 2011). In particular, those AGNs presenting strong Si-absorption features are often found to be hosted in highly inclined and/or merging galaxies (Deo et al. 2007, 2009). For some host-galaxy types and inclinations, the dust extinction may be so overwhelming that it has the ability to completely obscure an AGN (e.g., at optical and even mid-IR wavelengths; Goulding & Alexander 2009). Indeed, the mid-IR AGN emission in the late-type edge-on AGN NGC 4945 is almost entirely obscured based on *Spitzer*-IRS spectroscopy. Hence, in this section we test for a link between the observed mid-IR extinction and the properties of the host galaxy in Compton-thick AGNs.

In Figure 2, we highlight the optical classifications and host-galaxy inclinations for the Compton-thick AGN sample.[8] As noted previously, each of the 20 Compton-thick AGNs are hosted in late-type (S0–Scd) or irregular/merging galaxies. From stacked mid-IR spectra, we find that the galaxies classified optically as Seyferts (i.e., using standard optical emission-line diagnostic diagrams) have lower average apparent dust extinction ($S_{9.7} \sim 0.14$) than the Compton-thick AGNs hosted in the optically classified low-ionization nuclear emission-line regions (LINERs, i.e., sources with optical spectra characteristic of LINERs) and H II galaxies ($S_{9.7} \sim 0.55$). This dichotomy between apparent dust extinction and galaxy classification provides further evidence that the optical class may be influenced by high levels of intervening dust in the host galaxy. Additionally, we show that Compton-thick AGNs hosted in face-on (low-inclination) galaxies have mid-IR spectra exhibiting little or no apparent dust extinction ($S_{9.7} \sim 0.19$). By contrast, Compton-thick AGNs hosted in edge-on and/or merging systems have significantly greater dust extinction ($S_{9.7} \sim 0.96$, see Table 2), clearly suggesting that the Si-absorption features observed at mid-IR wavelengths have an extranuclear origin.

There are also three optically classified Seyferts (NGC 3281, NGC 4939, Circinus) within our Compton-thick sample which have larger Si-absorption features ($S_{9.7} \sim 0.8$–1.5) than would necessarily be expected given their moderate inclination angles ($b/a \sim 0.5$). Visual inspection of optical images used to derive the morphological classifications shows that these three Compton-thick AGNs have disturbed nuclear morphologies and/or dust lanes aligned along the galaxy nucleus. These additional extranuclear features may provide further regions of cool dust and, hence, larger Si-absorption strengths. Taken together, these results suggest that the dominant source of dust extinction observed at mid-IR wavelengths is not necessarily linked with an obscuring torus, but instead is arising from extended kilo-parsec-scale regions which lie far outside the expected dust-sublimation region of an accreting SMBH. Indeed, this galactic scale origin for the cool dust, which is required to produce deep Si-absorption features, is consistent with the wide range of $S_{9.7}$ observed in nearby starburst-dominated ultraluminous IR galaxies (e.g., Spoon et al. 2007; Desai et al. 2007; Farrah et al. 2008).

Despite our relatively small sample of sources, the 20 Compton-thick AGNs considered here cover a wide range of apparent dust-extinction values, $S_{9.7} \sim 0.0$–1.7. However, in Figure 2 we note a clear dearth of sources with $S_{9.7} > 0.3$ and $N_{\rm H} > 5 \times 10^{24}$ cm^{-2}. AGNs in this regime are likely to be heavily obscured at both mid-IR and optical wavelengths due, in part, to large quantities of intervening dust within the host galaxy, as

Table 2
Stacked Properties of Compton-thick AGNs

Sub-sample (1)	$S_{9.7}$ (2)	AGN:SB (3)
All sources	0.36	0.62
Optical Seyfert[a]	0.14	0.83
Optical LINER/H II[a]	0.55	0.43
Face-on/intermediate inclination	0.19	0.75
Edge-on inclination or merger	0.96	0.44

Notes. [1]Host-galaxy properties of sub-sample of main Compton-thick AGN sample; [2]average depth of Si-absorption feature ($S_{9.7}$) within stacked mid-IR spectra of sub-sample, measured using `DecompIR`; [3]AGN–starburst ratio derived from decomposition of stacked mid-IR spectra using `DecompIR` (AGN-dominated = 1).
[a] Excluding QSOs.

[8] The host-galaxy inclination angles are derived from the major–minor axis ratio as defined in the Third Reference Catalog of Bright Galaxies (de Vaucouleurs et al. 1991).

well as being heavily obscured at X-ray energies due to large gas columns within the torus. Such heavily obscured AGNs are still not robustly identified in the nearby universe. Observational expectations are that the numbers of Compton-thick AGNs with $N_{\rm H} \sim (1–5) \times 10^{24}$ cm^{-2} and $N_{\rm H} > 5 \times 10^{24}$ cm^{-2} are roughly constant (e.g., Risaliti et al. 1999; Salvati & Maiolino 2000). Based on the $S_{9.7}$–$N_{\rm H}$ distribution of our Compton-thick AGN sample, we should expect ≈6–8 sources in this "heavily obscured" parameter space; however, we find only one source, suggesting $\gtrsim$80% still remain unidentified in the nearby universe. From the sources currently identified with $S_{9.7} > 0.5$, we expect the majority of the "heavily obscured" systems to be optically unidentified due to large quantities of host-galaxy dust as well as being starburst dominated in the mid-IR. Hence, they will still remain unidentified in high-redshift multi-wavelength blank-field surveys. This will potentially cause a bias in our current perceived view of the heavily obscured AGN population and their place in galaxy evolution models.

As we have shown, the Si-absorption features in many edge-on Compton-thick AGNs appear to be unassociated with the dusty torus surrounding the central engine; we therefore cannot use these sources to constrain theoretical models for the AGN infrared emission. However, based on our results those Compton-thick AGNs hosted in face-on galaxies appear relatively unobscured in the mid-IR with $S_{9.7} \sim$ 0–0.3. Such AGNs are unlikely to have significant host-galaxy dust extinction along the line of sight; hence, any observed Si-absorption will be intrinsic to the torus. For a sensible (physical) range of AGN torus parameters (see Table 1 of Fritz et al. 2006; Table 1 of Schartmann et al. 2008), clumpy-torus models (e.g., Nenkova et al. 2002; Schartmann et al. 2008), whereby the dust is randomly distributed in discrete dust clouds, predict similarly weak Si-absorption ($S_{9.7} < 0.3$) for optically thick edge-on ($i = 90°$) tori. By contrast, uniform torus models (e.g., Pier & Krolik 1992; Fritz et al. 2006) predict large silicate features ($S_{9.7} \gg 1$) for similar input parameters. Indeed, for a Compton-thick system, uniform torus models reproduce $S_{9.7} \sim 0$ only when invoking a steep dust-density gradient across an extremely compact ($R_{\rm max}/R_{\rm min} \ll 30$) and somewhat unphysical torus. Therefore, under the paradigm of a clumpy torus, we suggest that the additional Si-absorption measured in those Compton-thick AGNs which are hosted in edge-on host galaxies becomes entirely consistent with extinction arising from dust which is distributed at very large radii (≫ parsecs) within the main host galaxy. In light of these findings, in Figure 3 we present a schematic diagram of the effect of the host-galaxy inclination and morphology on the observed mid-IR Si-absorption feature.

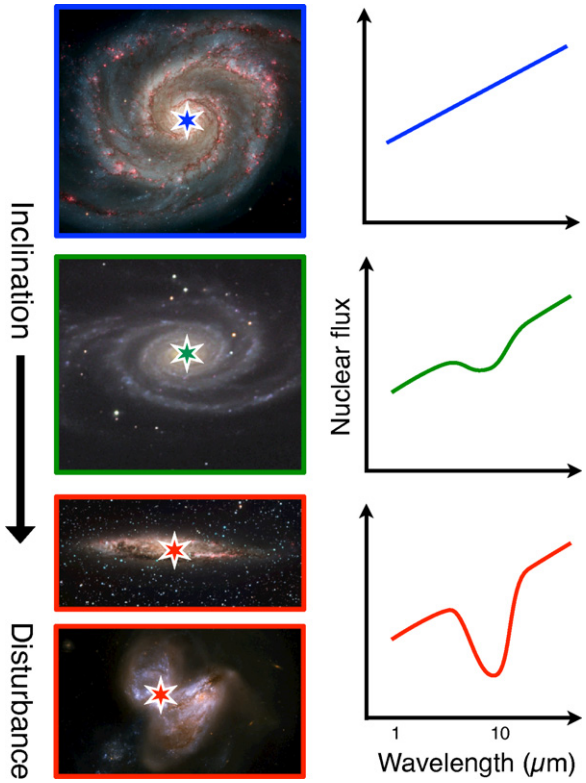

Figure 3. Schematic diagram illustrating the effect of host-galaxy inclination (and morphology disturbance) on the perceived dust extinction at mid-IR wavelengths. Based on the effects presented here, the strength of the Si-absorption feature at $\lambda \sim 9.7\,\mu$m qualitatively appears to increase with increasing galaxy inclination, i.e., consistent with the view that the obscuring dust which dominates the mid-IR extinction features arises only from within the host galaxy. Image credits, from top: NGC 5194: NASA and the Hubble Heritage Team (STSci/AURA); NGC 4939: Adam Block/NOAO/AURA/NSF; NGC 4945: ESO; Arp 299: NASA and the Hubble Heritage Team (STSci/AURA).

(A color version of this figure is available in the online journal.)

4. SUMMARY AND CONCLUSIONS

We have investigated mid-IR dust extinction in all hard X-ray ($E > 10$ keV) detected, bona fide Compton-thick ($N_{\rm H} \gtrsim 1.5 \times 10^{24}$ cm^{-2}) AGNs in the nearby universe to constrain the dominant source of attenuating dust in heavily obscured AGNs and build a more complete understanding of Compton-thick AGNs at mid-IR wavelengths. We measured Si-absorption features at 9.7 μm in archival low-resolution ($R \sim$ 57–127) mid-IR *Spitzer*-IRS spectroscopy to infer the attenuating dust column in these highly gas absorbed systems and determine the average mid-IR properties of Compton-thick AGNs. We found that the mid-IR SEDs of Compton-thick AGNs are diverse, and only in a minority of sources (9/20) do we find strong Si-absorption features ($S_{9.7} \gtrsim 0.5$). In turn, this suggests that sample selection based solely on the mid-IR absorption features may miss $\gtrsim$80% of Compton-thick AGNs. From analysis of the average mid-IR spectrum, we find that Compton-thick AGNs are characterized by roughly equal (40:60 ratio) quantities of starburst and AGN components which is only mildly dust obscured ($S_{9.7} \sim 0.36 \pm 0.04$, $A_V \approx$ 3.9–4.9), i.e., *average* dust-extinction levels which are consistent with those which are observed in host-galaxy star-forming regions. Furthermore, the high levels of star formation observed in these Compton-thick AGNs appear to be a feature specific to the most heavily obscured AGNs in the nearby universe. If such a trend continues toward higher redshifts, then infrared photometric and X-ray surveys which focus on the detection of power-law components to infer AGN activity within a source (e.g., Daddi et al. 2007; Donley et al. 2007, 2008) will be partially biased against the detection of a significant proportion of the Compton-thick AGN population and hence may still miss the majority of the most heavily obscured AGNs.

We compared $N_{\rm H}$ and $S_{9.7}$ in Compton-thick AGNs, and find no significant correlation between these two measures of apparent obscuration. We find that the most heavily attenuated sources ($S_{9.7} \gtrsim 0.5$) appear to be hosted in galaxies with visible dust lanes, disturbed morphologies, and/or galaxies which are highly inclined along the line of sight. By contrast, we show that sources hosted in face-on galaxies present only weak dust-extinction features ($S_{9.7} \sim$ 0–0.3). A similarly narrow range in Si-absorption is predicted by those theoretical torus models

which invoke clumpy distributions for the obscuring material. We suggest that the deeper silicate features ($S_{9.7} \gtrsim 0.5$), which are observed in only a minority of Compton-thick AGNs ($\approx$40%), arise from intervening dust at much larger scales than predicted for a torus (i.e., from within the host galaxy). When combined with previous investigations, this provides further evidence that the obscuring cool dust, which dominates the extinction seen at mid-IR (and optical) wavelengths, may not necessarily be cospatial with a gas-rich central torus.

The authors thank the anonymous referee for their timely and considered report which has allowed us to clarify and improve several aspects of the manuscript. We are also grateful to G. Risaliti for helpful discussions. This work was partially supported by NASA grants 13637399 and AR8-9017X. D.M.A. acknowledges funding from the Science and Technologies Funding Council. F.E.B. acknowledges support from Basal-CATA (PFB-06/2007) and CONICYT-Chile (FONDECYT 1101024 and ALMA-CONICYT 31100004). This work is based on observations made with the *Spitzer Space Telescope* and has made use of the NASA/IPAC Infrared Science Archive which are operated by the Jet Propulsion Laboratories, Californian Institute of Technology under contract with NASA.

Facility: Spitzer (IRS)

REFERENCES

Alexander, D. M., Bauer, F. E., Brandt, W. N., et al. 2011, ApJ, 738, 44
Alexander, D. M., Chary, R., Pope, A., et al. 2008, ApJ, 687, 835
Alonso-Herrero, A., Ramos Almeida, C., Mason, R., et al. 2011, ApJ, 736, 82
Antonucci, R. 1993, ARA&A, 31, 473
Asmus, D., Gandhi, P., Smette, A., Hönig, S. F., & Duschl, W. J. 2011, A&A, 536, A36
Awaki, H., Terashima, Y., Higaki, Y., & Fukazawa, Y. 2009, PASJ, 61, 317
Ballo, L., Braito, V., Della Ceca, R., et al. 2004, ApJ, 600, 634
Bassani, L., Dadina, M., Maiolino, R., et al. 1999, ApJS, 121, 473
Bassani, L., Malizia, A., Stephen, J. B., & INTEGRAL AGNs Survey Team. 2007, in Proc. VI INTEGRAL Workshop, The Obscured Universe, ed. S. Grebenev, R. Sunyaev, & C. Winkler (ESA Special Publication, Vol. 622; Noordwijk: ESA), 165
Beckmann, V., Soldi, S., Shrader, C. R., Gehrels, N., & Produit, N. 2006, ApJ, 652, 126
Braito, V., Della Ceca, R., Piconcelli, E., et al. 2004, A&A, 420, 79
Braito, V., Reeves, J. N., Della Ceca, R., et al. 2009, A&A, 504, 53
Brandl, B. R., Bernard-Salas, J., Spoon, H. W. W., et al. 2006, ApJ, 653, 1129
Cappi, M., Bassani, L., Comastri, A., et al. 1999, A&A, 344, 857
Collinge, M. J., & Brandt, W. N. 2000, MNRAS, 317, L35
Comastri, A., Gilli, R., Vignali, C., et al. 2007, Prog. Theor. Phys. Suppl., 169, 274
Comastri, A., Ranalli, P., Iwasawa, K., et al. 2011, A&A, 526, L9
Daddi, E., Alexander, D. M., Dickinson, M., et al. 2007, ApJ, 670, 173
Dasyra, K. M., Georgantopoulos, I., Pope, A., & Rovilos, M. 2011, in SF2A-2011: Proc. Annual Meeting of the French Society of Astronomy and Astrophysics, ed. G. Alecian, K. Belkacem, R. Samadi, & D. Valls-Gabaud, 91
Della Ceca, R., Ballo, L., Tavecchio, F., et al. 2002, ApJ, 581, L9
Della Ceca, R., Severgnini, P., Caccianiga, A., et al. 2008, Mem. Soc. Astron. Ital., 79, 65
Deo, R. P., Crenshaw, D. M., Kraemer, S. B., et al. 2007, ApJ, 671, 124
Deo, R. P., Richards, G. T., Crenshaw, D. M., & Kraemer, S. B. 2009, ApJ, 705, 14
Desai, V., Armus, L., Spoon, H. W. W., et al. 2007, ApJ, 669, 810
de Vaucouleurs, G., de Vaucouleurs, A., Corwin, H. G., Jr., et al. 1991, Third Reference Catalogue of Bright Galaxies, Vols. 1–3 (Berlin: Springer)
Donley, J. L., Rieke, G. H., Pérez-González, P. G., & Barro, G. 2008, ApJ, 687, 111
Donley, J. L., Rieke, G. H., Pérez-González, P. G., Rigby, J. R., & Alonso-Herrero, A. 2007, ApJ, 660, 167
Draine, B. T. 2003, ARA&A, 41, 241
Draine, B. T., & Li, A. 2007, ApJ, 657, 810
Dullemond, C. P., & van Bemmel, I. M. 2005, A&A, 436, 47
Efstathiou, A., & Rowan-Robinson, M. 1995, MNRAS, 273, 649
Farrah, D., Lonsdale, C. J., Weedman, D. W., et al. 2008, ApJ, 677, 957
Feruglio, C., Daddi, E., Fiore, F., et al. 2011, ApJ, 729, L4
Fitzpatrick, E. L. 1985, ApJ, 299, 219
Fritz, J., Franceschini, A., & Hatziminaoglou, E. 2006, MNRAS, 366, 767
Fukazawa, Y., Iyomoto, N., Kubota, A., Matsumoto, Y., & Makishima, K. 2001, A&A, 374, 73
Gandhi, P., Horst, H., Smette, A., et al. 2009, A&A, 502, 457
Georgantopoulos, I., Dasyra, K. M., Rovilos, E., et al. 2011, A&A, 531, A116
Gilli, R., Su, J., Norman, C., et al. 2011, ApJ, 730, L28
Goulding, A. D. 2010, PhD thesis, Durham Univ., UK
Goulding, A. D., & Alexander, D. M. 2009, MNRAS, 398, 1165
Goulding, A. D., Alexander, D. M., Lehmer, B. D., & Mullaney, J. R. 2010, MNRAS, 406, 597
Goulding, A. D., Alexander, D. M., Mullaney, J. R., et al. 2011, MNRAS, 411, 1231
Granato, G. L., & Danese, L. 1994, MNRAS, 268, 235
Granato, G. L., Danese, L., & Franceschini, A. 1997, ApJ, 486, 147
Guainazzi, M., Matt, G., Brandt, W. N., et al. 2000, A&A, 356, 463
Hao, L., Weedman, D. W., Spoon, H. W. W., et al. 2007, ApJ, 655, L77
Hönig, S. F., Kishimoto, M., Gandhi, P., et al. 2010, A&A, 515, A23
Iwasawa, K., Fabian, A. C., & Matt, G. 1997, MNRAS, 289, 443
Iwasawa, K., Matt, G., Fabian, A. C., et al. 2001, MNRAS, 326, 119
Iyomoto, N., Fukazawa, Y., Nakai, N., & Ishihara, Y. 2001, ApJ, 561, L69
Lagos, C. D. P., Padilla, N. D., Strauss, M. A., Cora, S. A., & Hao, L. 2011, MNRAS, 414, 2148
Levenson, N. A., Heckman, T. M., Krolik, J. H., Weaver, K. A., & Życki, P. T. 2006, ApJ, 648, 111
Levenson, N. A., Sirocky, M. M., Hao, L., et al. 2007, ApJ, 654, L45
Luo, B., Brandt, W. N., Xue, Y. Q., et al. 2011, ApJ, 740, 37
Maiolino, R., Marconi, A., Salvati, M., et al. 2001, A&A, 365, 28
Maiolino, R., Salvati, M., Bassani, L., et al. 1998, A&A, 338, 781
Malaguti, G., Palumbo, G. G. C., Cappi, M., et al. 1998, A&A, 331, 519
Malkan, M. A., Gorjian, V., & Tam, R. 1998, ApJS, 117, 25
Marinucci, A., Risaliti, G., Wang, J., et al. 2012, MNRAS, 423, L6
Markwardt, C. B., Tueller, J., Skinner, G. K., et al. 2005, ApJ, 633, L77
Mason, R. E., Levenson, N. A., Shi, Y., et al. 2009, ApJ, 693, L136
Matt, G., Fabian, A. C., Guainazzi, M., et al. 2000, MNRAS, 318, 173
Matt, G., Guainazzi, M., Frontera, F., et al. 1997, A&A, 325, L13
Matt, G., Guainazzi, M., Maiolino, R., et al. 1999, A&A, 341, L39
Mullaney, J. R., Alexander, D. M., Goulding, A. D., & Hickox, R. C. 2011, MNRAS, 414, 1082
Mullaney, J. R., Alexander, D. M., Huynh, M., Goulding, A. D., & Frayer, D. 2010, MNRAS, 401, 995
Mushotzky, R. F., Done, C., & Pounds, K. A. 1993, ARA&A, 31, 717
Nardini, E., & Risaliti, G. 2011, MNRAS, 415, 619
Nenkova, M., Ivezić, Ž., & Elitzur, M. 2002, ApJ, 570, L9
Nenkova, M., Sirocky, M. M., Nikutta, R., Ivezić, Ž., & Elitzur, M. 2008, ApJ, 685, 160
Nikutta, R., Elitzur, M., & Lacy, M. 2009, ApJ, 707, 1550
Norman, C., Hasinger, G., Giacconi, R., et al. 2002, ApJ, 571, 218
Pier, E. A., & Krolik, J. H. 1992, ApJ, 401, 99
Pier, E. A., & Krolik, J. H. 1993, ApJ, 418, 673
Risaliti, G., Maiolino, R., & Salvati, M. 1999, ApJ, 522, 157
Risaliti, G., Miniutti, G., Elvis, M., et al. 2009a, ApJ, 696, 160
Risaliti, G., Nardini, E., Salvati, M., et al. 2011, MNRAS, 410, 1027
Risaliti, G., Salvati, M., Elvis, M., et al. 2009b, MNRAS, 393, L1
Salvati, M., & Maiolino, R. 2000, in Large Scale Structure in the X-Ray Universe, ed. M. Plionis & I. Georgantopoulos (Paris: Atlantisciences), 277
Sazonov, S., Revnivtsev, M., Krivonos, R., Churazov, E., & Sunyaev, R. 2007, A&A, 462, 57
Schartmann, M., Meisenheimer, K., Camenzind, M., Wolf, S., & Henning, Th. 2005, A&A, 437, 861
Schartmann, M., Meisenheimer, K., Camenzind, M., et al. 2008, A&A, 482, 67
Shi, Y., Rieke, G. H., Hines, D. C., et al. 2006, ApJ, 653, 127
Siebenmorgen, R., & Krügel, E. 2007, A&A, 461, 445
Smith, J. D. T., Draine, B. T., Dale, D. A., et al. 2007, ApJ, 656, 770
Spoon, H. W. W., Marshall, J. A., Houck, J. R., et al. 2007, ApJ, 654, L49
Sturm, E., Schweitzer, M., Lutz, D., et al. 2005, ApJ, 629, L21
Turner, T. J., Perola, G. C., Fiore, F., et al. 2000, ApJ, 531, 245
Ueda, Y., Eguchi, S., Terashima, Y., et al. 2007, ApJ, 664, L79
Vignali, C., & Comastri, A. 2002, A&A, 381, 834
Vignati, P., Molendi, S., Matt, G., et al. 1999, A&A, 349, L57
Wang, J., Risaliti, G., Fabbiano, G., et al. 2010, ApJ, 714, 1497
Wu, Y., Charmandaris, V., Huang, J., Spinoglio, L., & Tommasin, S. 2009, ApJ, 701, 658